

Exploration of the ACOPF Feasible Region for the Standard IEEE Test Set

Optimal Power Flow Paper 6

Staff paper by
Aaron Schecter
Richard P O'Neill

February 2013

The views presented are the personal views of the authors and not the Federal Energy Regulatory Commission or any of its Commissioners.

0
y

-1

-2

$5\pi - \frac{4\pi}{3}$

$-\pi$

$-\frac{2\pi}{3}$

$-\frac{\pi}{3}$

x

0

$\frac{\pi}{3}$

$\frac{2\pi}{3}$

π

Exploration of the ACOPF Feasible Region for the Standard IEEE Test Set

Optimal Power Flow Paper 6

Aaron Schecter and Richard P O'Neill

aschec@gmail.com richard.oneill@ferc.gov

February 2013

Abstract and Executive Summary

The goal of our investigation is to gain some perspective on how non-convex the feasible region of the Alternating Current Optimal Power Flow (ACOPF) problem is. First, we will develop a metric for comparing how infeasible different solutions are. The set-up for this examination will be to generate convex combinations of feasible points, and determine how “far” these new points are from the feasible region. We propose a metric based on the relative two norm. This value will be compared over various regions around the optimal solution. Second, we would like to determine how elastic the area around the global optimum is; in other words, we will determine the largest range of values the optimization variables can take, given a small perturbation from the global solution. In doing so, we will find the elasticity of all optimization variables, which could give us insight into the structure of the feasible region. Finally, we will examine the two dimensional relationships between the optimization variables and the objective function value.

Index Terms—Optimal Power Flow, Feasible Region, Solution Space, Local Solutions, Elasticity

Disclaimer: The views presented are the personal views of the authors and not the Federal Energy Regulatory Commission or any of its Commissioners.

Table of Contents

Nomenclature1

1. Introduction	1
2. Feasible Region Of The Acopf Problem Ac Flow Equations	2
3. Elasticity Near The Optimal Solution	3
4. Fixed-Variable Optimizationacopf Formulation	5
5. Conclusions	7
References	7

NOMENCLATURE

Indices

n, m	Nodes
k	Lines
g	Generators

Variables

v_n	Voltage at Bus n
P_g	Real Power at Generator g
Q_g	Reactive Power at Generator g
θ_n	Voltage Angle at Bus n
θ_{nm}	Voltage difference (i.e. $\theta_n - \theta_m$)
U	Uniform Random Variable
x	Vector of Optimization Variables (i.e. $x = [\theta, V, P, Q]$)
$x^{(r)}$	Vector of Optimization Variables from Random Objective Function
$x^{(c)}$	Vector of Optimization Variables from Convex Combination

Parameters

V^{\min}, V^{\max}	Minimum and Maximum Voltage Magnitude Vector
P^{\min}, P^{\max}	Minimum and Maximum Real Power Capacity Vector
Q^{\min}, Q^{\max}	Minimum and Maximum Reactive Power Capacity Vector
$\theta_{nm}^{\min}, \theta_{nm}^{\max}$	Minimum and Maximum Angle Difference Between Bus n and m
c_{gi}	i^{th} Order Cost Term for Generator g
G_{nmk}	Electrical Conductance from Bus n to m along Line k <i>Note: For our purposes, the transmission lines are numbered 1 through K</i>
B_{nmk}	Electrical Susceptance from Bus n to m along Line k

Sets

N	Set of Nodes
G	Set of Generators
K	Set of Transmission Lines
S	Set of Constraints

I. INTRODUCTION

The problem of finding an optimal power flow solution in a network proves especially challenging from a computational standpoint. The ACOPF problem is an example of a non-linear programming problem over a non-convex feasible region. Today's optimization algorithms generally rely on the Karush-Kuhn-Tucker (KKT) conditions for optimality, but this set of criteria assumes a convex region. Previous investigation of the ACOPF problem suggests that the region is suitably convex [3] for the application of the KKT conditions; however, the region is in fact non-convex and therefore the KKT conditions fail to guarantee global optimality. In fact, modern algorithmic methods still do not guarantee convergence to a global optimum. One approach that does not rely on the KKT conditions is the method proposed in [4], which establishes an algorithm based on semi-definite programming that results in a duality gap of zero.

In general, it can be shown that there are a large number of physically feasible load flow solutions [5] and thus numerous local optima. As a result, the issue of convexity becomes important for both accuracy and reliability purposes. In this paper, we establish some basic characteristics of these problems using the IEEE standard test suite [1] and further contribute to the discussion of their structure.

The first segment of our investigation focuses on points that are nearly feasible. In other words, if we examine some convex combination of two known feasible points, to what degree will this new point be infeasible, if it is in fact infeasible. Because the region is non-convex, our expectation is not to find many feasible combinations; however, if we find only small deviations from the feasible region, that would support the suitably convex hypothesis.

The second area of focus is the elasticity of the optimization variables. Rather than look only at the predefined limits on the variables, we examine the effective limits. In other words, what are the extreme values of each variable, such that overall feasibility is maintained. To refine this search to a meaningful scope, we only consider feasible points that correspond to objective function values within one percent of the global optimum. Therefore, our examination centers on the area around the global optimum and we seek to establish how flat that region of the feasible set is.

Finally, we determine the behavior of the optimization variables across their range of feasible values. In particular, we will investigate the pairwise relationships between a single variable's value and the objective function value. The nature of these relationships should lend some insight into how changes in the power flow can affect the subsequent cost, as well as characterize the relative convexity of the region around the optimum. Additionally, by iterating through all of the feasible values for each variable, we should expect to find some local optima corresponding to those power flow profiles.

II. FEASIBLE REGION OF THE ACOPF PROBLEM

Our procedure is two stage: first, we solve for a global optimum of the ACOPF problem. A solution is considered globally optimal in this paper if it satisfies the first order KKT conditions to a default tolerance of 10^{-6} . Note that this is a necessary but not sufficient condition for optimality. The problem is solved in the polar formulation:

$$\min f(x) = \sum_{g \in G} c_{g2} P_g^2 + c_{g1} P_g + c_{g0} \quad (1)$$

$$\text{s. t. } P_n = \sum_{m \in N} v_n v_m (G_{nmk} \cos \theta_{nm} + B_{nmk} \sin \theta_{nm}) \quad (2)$$

$$Q_n = \sum_{m \in N} v_n v_m (G_{nmk} \sin \theta_{nm} - B_{nmk} \cos \theta_{nm}) \quad (3)$$

$$P \leq P^{\max} \quad (4)$$

$$P^{\min} \leq P \quad (5)$$

$$Q \leq Q^{\max} \quad (6)$$

$$Q^{\min} \leq Q \quad (7)$$

$$V^{\min} \leq V \leq V^{\max} \quad (8)$$

We will refer to the constraint set as $S = \{(2), (3), \dots, (8)\}$. In the typical polar formulation of the ACOPF problem, we would also include line constraints and voltage angle constraints. However, the IEEE standard test problems are by default not

bounded by these constraints; the input data for branch and angle limits are effectively infinite. Therefore, these constraints are not included in our formulation. The original problem (1),..., (8) is solved using the solver `fmincon` in the MATLAB package `MATPOWER` (Version 4.1) [2].

Next, in an attempt to quantify how non-convex the feasible region is, we consider the mid-point of two feasible points and test it for feasibility. For each of the cases (14, 30, 57, 118, and 300 bus), we substitute the default objective function with a randomized linear cost function. In other words, (1) is replaced with the objective function

$$f(x) = \sum_{g \in G} U c_{g1} P_g \quad (9)$$

where U is a uniform random variable, and c_{g1} is the problem's default linear cost term. All other cost terms are ignored. We minimize this objective function over our region S and obtain a local optimal solution that will be on the boundary of S , by first order optimality conditions (Procedure 1, Step 1). Next, we examine all of the pairwise mid-points. To determine feasibility, we calculate the minimum relative ℓ_2 -norm of the convex combination and a feasible point from the set S (Procedure 1, Step 5); a result of zero indicates that the convex combination is a feasible point. Since the point that minimizes the Euclidean distance metric is also the minimizer for the ℓ_2 -norm, we use it for smoothness considerations. We examine the relative magnitude in the ℓ_2 -norm so that our objective function value serves as a more meaningful metric; it is easier to compare "how infeasible" different solutions are when their values are scaled by the optimal values. Our process is described in Procedure 1.

Procedure 1: Test for Convexity

1. Let (P) denote the optimization problem

$$\min f(x) = \sum_{g \in G} U c_{g1} P_g \quad (10)$$

$$\text{s. t. } x \in S, U \sim \text{Uniform}(0, 2)$$

2. Solve (P) 100 times

3. Let $x_i^{(r)}$ be the i th solution

4. For each pair of solutions $i \neq j$

$$x_{ij}^{(c)} = 0.5x_i^{(r)} + 0.5x_j^{(r)} \quad (11)$$

5. Solve the following $\forall i, j$ pairs, $i \neq j$

$$\min g(x) = \sum_{g \in G} \frac{(P_{g,ij}^{(c)} - P_g)^2}{|P^*|} + \sum_{g \in G} \frac{(Q_{g,ij}^{(c)} - Q_g)^2}{|Q^*|} \quad (12)$$

$$+ \sum_{n \in N} \frac{(v_{n,ij}^{(c)} - v_n)^2}{|v^*|}$$

$$\text{s.t. } x \in S$$

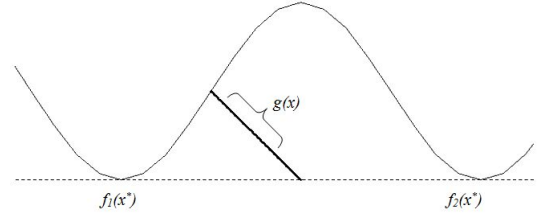
6. Report the values of $g(x^*)$ from (12)
-

To determine the convexity of the region around the global solution, we set U so that U is drawn from the `Uniform(0, 2)` distribution. The results of this procedure are summarized in Table 1. After doing so, we restrict the region to $U \sim \text{Uniform}(0.99, 1.01)$. By doing so, we should restrict our randomized local solutions to a much tighter region of the feasible set. The results of this change are summarized in Table 2.

Figure 1 illustrates the value we are trying to minimize. In two dimensions, we would simply try to minimize the Euclidean

distance between the midpoint of two feasible points ($f_1(x^*)$ and $f_2(x^*)$) and the feasible set S .

Figure 1. A two-dimensional illustration of the infeasibility metric we seek to minimize



A. Convex Combination Feasibility

For our convex combination procedure, we report the mean and median values for each case, and we record the number of feasible points (objective function value of zero). To give some notion of how variable the differences are, we also report the maximum and minimum values of the objective function.

As we can see from Table I, none of the convex combinations are feasible points when the random variable is drawn from the `Uniform(0, 2)` distribution; additionally, there is no obvious correlation between size of the problem and "how non-convex" the constraint set is. In fact, the 300 bus case has the lowest values of our infeasibility metric; this implies that, relative to the variable values, the convex combinations of 300 bus case solutions are closest to known feasible points.

Table I
SUMMARY OF MIDPOINT FEASIBILITY TEST RESULTS, WITH RANDOM VARIABLE $U \in [0, 2]$

Case	Mean	Median	Feasible Points	Minimum	Maximum
14	0.542	0.512	0	0.29	1.595
30	0.47	0.455	0	0.336	0.823
57	0.66	0.643	0	0.341	1.178
118	1.39	1.335	0	0.648	2.704
300	0.082	0.082	0	0.062	0.105

Next, we restrict the objective function's variation by introducing a uniform random variable with a smaller range and repeat Procedure 1. Our results for the `Uniform(0.99, 1.01)` randomized objective function are as follows in Table II:

Table II
SUMMARY OF MIDPOINT FEASIBILITY TEST RESULTS, WITH RANDOM VARIABLE $U \in [0.99, 1.01]$

Case	Mean	Median	Feasible Points	Minimum	Maximum
14	0.551	0.522	0	0.292	1.535
30	0.468	0.453	0	0.329	0.806
57	0.686	0.673	0	0.424	1.071
118	1.469	1.466	0	0.501	2.473
300	0.077	0.078	0	0.050	0.103

Restricting the region of points does not have much of an impact on the mean and median ℓ_2 -norm. However, the minimum and maximum difference values do decrease. These

results suggest that on average, the midpoint between any two feasible points will be as infeasible as either point, regardless of our choice of points. This conclusion may give us some insight into the shape of S ; if the non-convexities of the feasible region were sharp, then we would see wider variation in the infeasibility metric as we moved the points closer together. However, if we produce similar values for different choices of random variables, then the notion of a flat feasible region becomes more tractable.

Aside from the midpoint, we look at a more general case of convex combinations:

$$x^{(c)} = \alpha x_1 + (1 - \alpha)x_2, \alpha \in [0, 1] \quad (13)$$

Generally speaking, as α approaches 0 (or 1), the convex combination of variables will become more similar to one of the two feasible points. Thus, we investigate how our infeasibility metric changes over different values of α . For this procedure, we repeat Procedure 1 with $U \sim \text{Uniform}(0.99, 1.01)$, but replace (11) with (13), and test at the following points: $\alpha = 0.05, 0.1, 0.15, 0.2, 0.25, 0.3, 0.35, 0.4, 0.45$. This test is performed for the 14 and 30 bus case; we report the following results in Table III:

Table III
RESULTS FOR INFEASIBILITY TEST AT VARIOUS ALPHA VALUES; MEAN RESULTS REPORTED FOR THE 14 AND 30 BUS CASES

Mean Infeasibility		
α	14 Bus	30 Bus
0.05	0.690	0.574
0.10	0.660	0.553
0.15	0.634	0.533
0.20	0.612	0.517
0.25	0.593	0.502
0.30	0.578	0.491
0.35	0.566	0.481
0.40	0.557	0.474
0.45	0.553	0.470
0.50	0.542	0.468

The results show that the convex combination that varies the least in our ℓ_2 -norm is the midpoint. In fact, as the convex combination favors one point over the other, the combination actually varies more from the feasible set. This relationship is illustrated by both the 14 and 30 bus case, with a nearly identical shape to the plots (Figure 2).

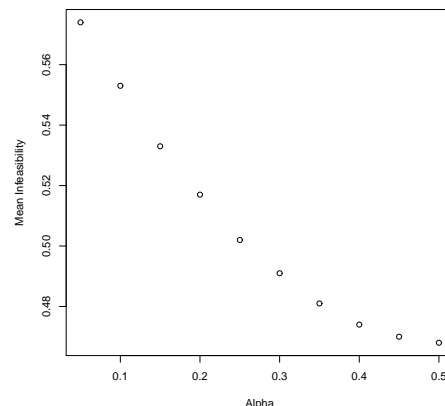
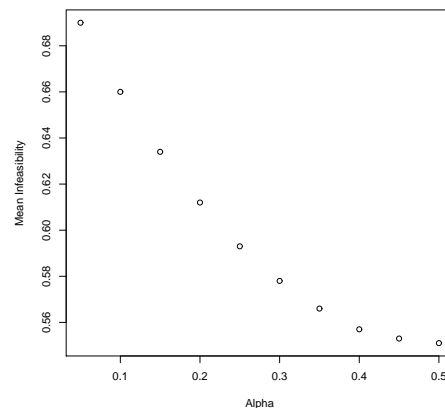
III. ELASTICITY NEAR THE OPTIMAL SOLUTION

Elasticity is a measure of the magnitude of change in a variable as a result of change in another variable. We will denote the elasticity in variable y with respect to variable x as:

$$E_{y,x} = \left| \frac{\Delta y/y}{\Delta x/x} \right| \quad (14)$$

For the ACOPT problem, we are interested in how greatly the optimization variables can change while maintaining an objective function value that is within 1% of the global optimum (Procedure 2, Step 3). Because the feasible region S is a non-convex set, we are interested in the elasticity as a measure of

Figure 2. A plot of Alpha level against mean infeasibility, 14 bus case (top) and 30 bus case (bottom)



how flat the area around the global optimum of problem (1) is; if in fact the area is highly elastic (flat), then it is possible that the non-convexities of S are not severe enough to force our algorithms into local optima.

To measure the elasticity, we calculate the absolute difference between the minimum and maximum values (Procedure 2, Step 4), divided by the magnitude of the optimal value, then divided by the allowed percentage change in the optimal objective function value (Procedure 2, Step 5). These problems were all solved in MATLAB using the non-linear solver `fmincon`, with tolerances for costs and constraint violations set at 10^{-6} . These problems were solved for every bus and every generator. The data used were the IEEE 14, 30, 57, 118, and 300 bus cases. Our process is described in Procedure 2.

Procedure 2: Compute Elasticity

For each case:

1. Solve for the optimal solution of (1)

$$x^* = [\theta^*, V^*, P^*, Q^*] \quad (15)$$

2. Find the corresponding objective function value

$$f(x^*) = \sum_{g \in G} c_{g2} P_g^{*2} + c_{g1} P_g^* + c_{g0} \quad (16)$$

3. Add new constraint to S

$$\begin{aligned} f(x) &\leq 1.01 f(x^*) \\ S' &= S \cup (17) \end{aligned} \quad (17)$$

4. Solve the new optimization problems

$$\min / \max v_n \quad (18)$$

subject to $x \in S'$

$$\min / \max P_g \quad (19)$$

subject to $x \in S'$

$$\min / \max Q_g \quad (20)$$

subject to $x \in S'$

5. Compute the elasticities

$$E_{v_n, f} = \frac{v_n^{\max} - v_n^{\min}}{v_n^*} / (0.01) \quad (21)$$

$$E_{P_g, f} = \frac{P_g^{\max} - P_g^{\min}}{P_g^*} / (0.01) \quad (22)$$

$$E_{Q_g, f} = \frac{|Q_g^{\max} - Q_g^{\min}|}{|Q_g^*|} / (0.01) \quad (23)$$

Table IV

THE RESULTS FOR THE TEST OF VARIABLE RANGES FOR THE 14 BUS CASE; MINIMUM, MAXIMUM, AND OPTIMAL VALUES ARE REPORTED

Variable	Minimum	Optimal	Maximum
v_1	0.969	1.06	1.06
v_2	0.945	1.041	1.048
v_3	0.94	1.016	1.047
v_4	0.94	1.014	1.026
v_5	0.94	1.016	1.025
v_6	0.959	1.06	1.06
v_7	0.950	1.046	1.052
v_8	0.94	1.06	1.06
v_9	0.951	1.044	1.051
v_{10}	0.951	1.039	1.045
v_{11}	0.958	1.046	1.049
v_{12}	0.945	1.045	1.045
v_{13}	0.942	1.04	1.041
v_{14}	0.94	1.024	1.029
P_1	156.308	194.327	231.296
P_2	19.074	36.719	54.366
P_3	1.99E-06	28.737	68.350
P_6	2.00E-08	0.0138	48.316
P_8	2.00E-06	8.491	59.668
Q_1	2.00E-08	0.0234	10
Q_2	-29.628	23.681	50
Q_3	2.00E-06	24.126	40
Q_6	-6	11.529	24
Q_8	-6	8.274	24

A. Test Ranges

We report the optimal value, maximum, and minimum value of each optimization variable for the 14 (Table IV) and 30 (Table V) bus problems. These results correspond to step 4 of Procedure 2 ((18), (19), and (20)). It should be noted that the default limits for voltage magnitude in the 14 bus case are [0.94, 1.06], while the limits for the 30 bus case are [0.95, 1.05]. Individual generator power limits were also left at their default values. These limits were not changed for the sake of easy replication. Interestingly, we see that while many of these variables have a wide range, the voltage magnitudes and real power generally do not span all feasible values, while reactive power can fluctuate across its entire spectrum. The likely cause is that reactive power costs are not included in the standard objective function, which is to minimize the cost of real power.

B. Elasticities

We report the elasticity of our optimization variables for the 14 and 30 bus cases, as calculated in Step 5 of Procedure 2 ((21), (22), and (23)) in Table VI.

Summarized in Table VII are the mean and median elasticities for each of the cases. The median was considered due to the high frequency of extreme values, which skew the mean. In the 14 bus case, there are particularly glaring discrepancies between the mean and median power (active and reactive) elasticities.

As we can see from Table VII, each variable has an elasticity much higher than 1. Reactive power is especially elastic, and is consistently more elastic than the other optimization variables. In the 57 bus case, however, reactive power is not significantly

more elastic than the other variables. In the 118 bus case, the median range of reactive power is more than 600% the magnitude of the optimal solution. Despite these large results for the 118 bus case, we observe that there is not a consistent trend between size of the problem and elasticity of the variables, similar to our findings regarding our infeasibility metric. The 57 bus case is the least elastic across all three types of variables, and the 300 bus case is the second least elastic. We can thus hypothesize that the size of the problem is not the driver of variable elasticities, and therefore does not directly affect the shape of the feasible region.

IV. FIXED-VARIABLE OPTIMIZATION

To determine the isolated affect of one variable on the overall objective function value, multiple optimization problems can be solved at various levels, and the changes in cost can be tracked. For the ACOPF problem, we fixed a single variable value (Procedure 3, Line 3), and performed the optimization using that variable as an additional constraint (Procedure 3, Line 5). As an output of this procedure, we will obtain a graphical representation of the relationship between various levels of the particular variable and objective function values. This process was completed for the IEEE 14, 30, and 57 bus cases. For the purposes of space, we will include a deeper look at the 14 bus case only. Our process is described more fully in Procedure 3:

Table V

THE RESULTS FOR THE TEST OF VARIABLE RANGES FOR THE 30 BUS CASE; MINIMUM, MAXIMUM, AND OPTIMAL VALUES ARE REPORTED

Variable	Minimum	Optimum	Maximum
v_1	0.951	0.983	1.05
v_2	0.951	0.979	1.059
v_3	0.961	0.977	1.041
v_4	0.961	0.977	1.039
v_5	0.955	0.971	1.042
v_6	0.961	0.973	1.034
v_7	0.950	0.963	1.028
v_8	0.95	0.961	1.022
v_9	0.955	0.991	1.039
v_{10}	0.951	1.000	1.043
v_{11}	0.955	0.991	1.039
v_{12}	0.954	1.018	1.05
v_{13}	0.95	1.066	1.1
v_{14}	0.95	1.007	1.045
v_{15}	0.951	1.01	1.05
v_{16}	0.954	1.003	1.04
v_{17}	0.95	0.996	1.037
v_{18}	0.95	0.994	1.035
v_{19}	0.95	0.988	1.03
v_{20}	0.95	0.99	1.033
v_{21}	0.95	1.009	1.05
v_{22}	0.951	1.016	1.059
v_{23}	0.95	1.026	1.1
v_{24}	0.95	1.017	1.05
v_{25}	0.968	1.044	1.05
v_{26}	0.95	1.027	1.033
v_{27}	0.983	1.069	1.069
v_{28}	0.963	0.982	1.037
v_{29}	0.962	1.05	1.05
v_{30}	0.95	1.039	1.039
P_1	25.624	41.51	61.989
P_2	38.768	55.362	79.893
P_{22}	12.114	22.733	34.043
P_{27}	10.058	39.948	55
P_{23}	0.925	16.3	30
P_{13}	0.93	16.206	33.79
Q_1	-20	-5.469	81.401
Q_2	-20	1.539	60
Q_{22}	-15	33.905	62.5
Q_{27}	-15	31.639	46.347
Q_{23}	-10	7.06	40
Q_{13}	-15	36.445	44.7

Table VI

RESULTS OF ELASTICITY CALCULATION; REPORTED ARE ELASTICITY VALUES FOR ALL OPTIMIZATION VARIABLES FROM THE 14 BUS (LEFT) AND 30 BUS (RIGHT) CASES

Variable	Elasticity
v_1	10.11
v_2	11.07
v_3	8.16
v_4	7.97
v_5	8.91
v_6	7.45
v_7	8.10
v_8	7.50
v_9	8.51
v_{10}	9.19
v_{11}	8.51
v_{12}	9.40
v_{13}	14.07
v_{14}	9.42
v_{15}	9.80
v_{16}	8.64
v_{17}	8.77
v_{18}	8.59
v_{19}	8.13
v_{20}	8.35
v_{21}	9.91
v_{22}	10.63
v_{23}	14.61
v_{24}	9.83
v_{25}	7.81
v_{26}	8.08
v_{27}	8.07
v_{28}	7.60
v_{29}	8.39
v_{30}	8.57
P_1	87.61
P_2	74.28
P_{22}	96.47
P_{27}	112.50
P_{23}	178.38
P_{13}	202.77
Q_1	1854.24
Q_2	5199.19
Q_{22}	228.58
Q_{27}	193.92
Q_{23}	708.18
Q_{13}	163.81

Variable	Elasticity
v_1	8.57
v_2	9.86
v_3	10.54
v_4	8.46
v_5	8.39
v_6	9.50
v_7	9.73
v_8	11.32
v_9	9.52
v_{10}	9.08
v_{11}	8.75
v_{12}	9.62
v_{13}	9.54
v_{14}	8.64
P_1	38.59
P_2	96.12
P_3	237.85
P_6	350625.54
P_8	702.71
Q_1	42733.22
Q_2	336.26
Q_3	165.80
Q_6	260.22
Q_8	362.59

Procedure 3: Fixed-Variable Optimization

For each case:

1. Select an optimization variable P_g (or Q_g, v_n)
2. Determine the range, $R_{P_g} = P_g^{\max} - P_g^{\min}$, of feasible values for the variable
3. Let $P_g = P_g^{\min} + c_i R_{P_g}$ for $i = 1, \dots, 100$ where $c_i = i/100$ (24)

4. Add new constraint to S
 $S'' = S \cup (24)$ (25)

5. Solve the optimization problem (1) under constraint set S''

6. Plot objective function value againsts values of P_g

Table VII

SUMMARY STATISTICS FOR OPTIMIZATION VARIABLE ELASTICITIES

Test Case		Voltage	Power	Reactive Power
14	Median	9.51	237.85	336.26
	Mean	9.40	70340.16	8771.62
30	Median	8.58	104.48	468.38
	Mean	9.12	125.33	1391.32
57	Median	2.88	102.49	243.15
	Mean	3.79	101.87	360.35
118	Median	11.02	499.33	676.37
	Mean	10.88	57053.86	4228.16
300	Median	7.80	137.19	229.32
	Mean	7.46	10712.25	3403.45

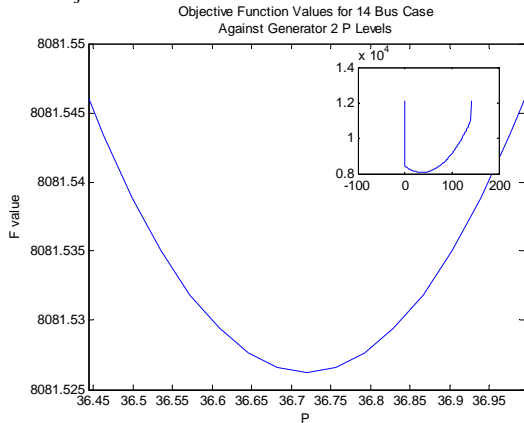
smooth relationships between their values and cost and are generally convex. On the whole, the majority of optimization variables fall into this category; their values with respect to the objective function are parabolic with minima at the global optimum. It should be noted that for visualization purposes, infeasible points (or points that failed to lead to a convergent solution) are designated with objective function value of $1.5f^*$,

A. Graphical Representations of the 14 Bus Problem

1) *Well Behaved Graphs*: We first report on the general class of variables that are “well-behaved”; in other words, they display

which serves as effectively infinite. For the inset graphs, we observe a “bucket” shape; this effect is caused by the values falling outside the feasible region. A “well-behaved” variable generally had a shape similar to Figure 3.

Figure 3. Real Power at Generator 2 plotted against Objective Function Value. The inset of the graph represents a plot over the full range of feasible values; the larger graph is a “zoomed-in” region focused on the 1% neighborhood of the optimal objective function value.



There are interesting observations to be made about the power, reactive power, and voltage profiles. The real power, since it is the driver of cost in the objective function, seems to have a very strong correlation with cost. Since our cost terms are quadratic, it makes sense that over the full range of values real power has a parabolic relationship to cost.

Reactive power, on the other hand, is rather flat. Conversely to real power, reactive power is not a factor in the objective function; the flat relationship we see corresponds well to our earlier findings regarding the highly elastic nature of reactive power values. However, the interesting aspect of the reactive power graph is that it appears quadratic in the immediate neighborhood of the global optimum. This behavior lends itself to a convex relationship.

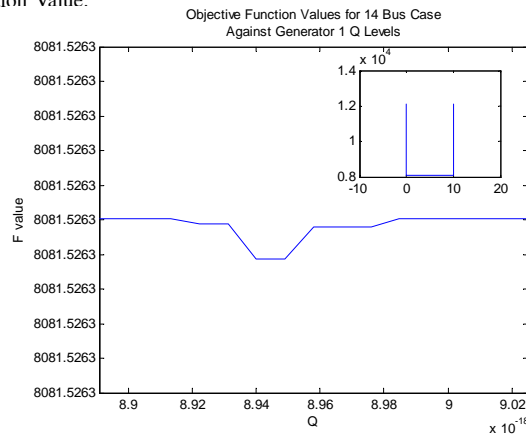
Like reactive power, voltage magnitude is also flat, which should be expected given its absence from the objective function. Unlike real power and reactive power, voltage magnitude does not display an even, symmetric curvature around the optimal value. Rather, most buses display a relatively flat curvature with voltage levels that are below optimal, while voltage magnitudes that are too high increase the cost almost exponentially. Also, it is interesting to note that, like in Figure 3, most voltages have their optimal value at the higher end of their feasible range.

2) *Irregular Graphs*: Some variables display irregular behavior with respect to cost, particularly in the form of infeasible points within the standard bounds. An examples of this can be seen in Figure 4:

In the case of power at generator 1, our algorithms find a single feasible point when power is fixed at 83% of its upper bound. However, between the 79th and 82nd percentage level, we fail to achieve convergence. In particular, our non-linear solver failed to converge after 400+ iterations and 10,000 function evaluations, while the 83% level converged in 8 iterations. This specific irregularity has no ready explanation.

For bus 12, the optimal solution is strictly less than the upper

Figure 4. Graphs of Reactive Power at Generator 1 Plotted Against Objective Function Value.



bound (1.06 in this case), yet is infeasible when pushed beyond the optimal value. In fact, with a 0.1% perturbation in the positive direction, our non-linear solver fails to find a solution after 500 iterations. It is unclear what aspect of the network topology contributes to this infeasibility.

V. CONCLUSIONS

At the conclusion of our investigation, we see no strong evidence to suggest that the ACOFP problem is nearly convex. However, many of our observations suggest that the problem has some convex properties, but too many irregularities to be considered reasonably convex.

Across every problem in the IEEE test set, we fail to find any feasible convex combinations of feasible points. Additionally, if the convex combination favors one point over the other, we find that our infeasibility metric increases. This result suggests that not only is the region non-convex, but very immediately so. If we look at our elasticity results, we see that our optimization variables can vary greatly without having a significant impact on the objective function value.

Combining this characteristic with our feasible point exploration, we can conclude that the region is globally flat but locally very dynamic for any constricted region. Our results lend support to the frequent observation of local optima; because the area around the true optimum is flat, solvers may quickly converge to values close to the optimum. However, the local topology would make it very easy for the solver to find a feasible, sub-optimal point and declare optimality.

Finally, our visual examination of the pair-wise relationships between variable values and cost suggest that many variables display smooth quadratic behavior, at least in the neighborhood of the optimal solution. However, the presence of some highly irregular points and behavior indicative of local optima contradicts the claim that the variables are convex in nature.

REFERENCES

- [1] “IEEE Power Systems Test Archive,” College of Engineering University of Washington [Online]. Available: <http://www.ee.washington.edu/research/pstca>.
- [2] R. D. Zimmerman, C. E. Murillo-Sánchez, and R. J. Thomas, “MATPOWER Steady-State Operations, Planning and Analysis Tools for Power Systems Research and Education,” *Power Systems*, IEEE Transactions on, vol. 26, no. 1, pp. 12-19, Feb. 2011.

- [3] J. Carpentier, "Contribution à l'étude du dispatching économique," Bulletin de la Société Française des Électriciens, ser. 8, vol. 3, pp. 431-447, 1962
- [4] Javad Lavaei, Steven H. Low, "Convexification of Optimal Power Flow Problem," Forty Eighth Annual Allerton Conference on Communication, Control, and Computing, Monticello, IL, Oct. 2010
- [5] A. Klos, J. Wojcicka, "Physical Aspects of the Nonuniqueness of Load Flow Solutions," Electrical Power and Energy Systems, 1991